COLORADO STATE UNIVERSITY
FORT COLLINS, COLORADO
80521

department of electrical engineering

ELECTROHYDRODYNAMIC HEAT PIPE RESEARCH

Research Report #4

July 1973

By

T. B. Jones and M. P. Perry

Department of Electrical Engineering

Colorado State University

Fort Collins, Colorado 80521

NASA Grant # NGR-06-002-127

Prepared for

Ames Research Center
National Aeronautics and Space Administration
Moffett Field, California 94035

This work was performed under the auspices of NASA/Ames Research Center, Grant # NGR-06-002-127. Mr. J. P. Kirkpatrick is the Technical Monitor.

The research program is being conducted by Dr. Thomas B. Jones, Assistant Professor of Electrical Engineering, Colorado State University, Ft. Collins, Colorado 80521.

ELECTROHYDRODYNAMIC HEAT PIPE RESEARCH

NASA CR-114646

Research Report #4

July 1973

By

T. B. Jones and M. P. Perry

Department of Electrical Engineering

Colorado State University

Fort Collins, Colorado 80521

NASA Grant # NGR-06-002-127

Prepared for

Ames Research Center

National Aeronautics and Space Administration

Moffett Field, California 94035

TABLE OF CONTENTS

CHAPTER		PAGE
I.	Introduction	1
II.	Theoretical Considerations	3
	A. Description of Goals	3
	B. Approximate Heat Pipe Conductance	3
	Heat Transfer in Laminar Flow	3
	Approximate Evaporator Conductance	6
	Other Contributions to Thermal Resistance	8
	Calculation of Heat Pipe Conductance	9
	C. Evaporator Groove Design	11
	Problem Definition	11
	Hydrodynamic Equations	14
	Boundary Conditions	16
	Burn-Out Condition	17
	Solution to Hydrodynamic Equations	18
	Comments on Maximum Heat Flux Into a Groove	23
	D. Discussion of Theoretical Results	23
	Heat Pipe Conductance and Groove Design	23
	Extension of Theoretical Results	24
III.	Capillary Feltmetal EHD Heat Pipe Experiment	27
IV.	Discussion	37
	A. Conclusions Based on Theoretical Results	37
	B. Experimental Results	38
	Heat Pipe Conductance	39
	Other Experimental Results	40
	C. Further General Discussion	40
ACKNOWLEDGEMENT		42
APPENDIX		43
REFERENCES		45

LIST OF FIGURES

FIGURE		PAGE
Figure 1a	Flat-Plate Evaporator and Condenser Configuration	7
Figure 1b	Rectangular Groove Geometry in Flat-Plate Evaporator and Condenser	7
Figure 2a	Fluid Configuration in a Groove	13
Figure 2b	Deep Groove Case, w<<d	13
Figure 3a	Maximum Heat Flux vs. Groove Width	20
Figure 3b	Maximum Heat Flux vs. Groove Width	21
Figure 3c	Maximum Heat Flux vs. Groove Width	22
Figure 4a	Triangular Groove Configuration	26
Figure 4b	Possible Cylindrical Groove Configuration	26
Figure 5a	Exploded View of Feltmetal Heat Pipe	28
Figure 5b	Cross-sectional View of Second Electro-hydrodynamic Heat Pipe Experiment	28
Figure 6a	Evaporator-Condenser Temperature vs. Tilt for Feltmetal EHD Heat Pipe Condenser Temperature = 49°C	32
Figure 6b	Evaporator-Condenser Temperature vs. Tilt for Feltmetal EHD Heat Pipe Condenser Temperature = 23°C	33
Figure 7	Feltmetal Heat Pipe Conductance vs. Input Power When Capillary Wick is Just Saturated with Liquid and No Voltage Applied	35

I. Introduction

Previous research reports in this series have considered the feasibility of electrohydrodynamic (EHD) heat pipes,[1] the entrainment limit in these devices,[2] and initial data obtained with the first experimental EHD heat pipe.[3] This present report covers more recent work performed on both experimental and theoretical fronts related to the research program.

In the first EHD heat pipe experiment,[3] a design was tested which employed a tent electromechanical flow structure for axial liquid flow and circumferential threaded grooves for surface distribution. The principal factor limiting the performance of the device was found to be the grooves which did not have sufficient pumping capability. As a consequence of this experiment, theoretical investigations have now been made of grooves and groove performance specifically for dielectric fluids. Both the rate of heat transfer from the evaporator surface and the groove pumping capacity have been studied. The theory should allow the optimal design of the grooves of future EHD heat pipes with respect to maximum heat throughputs and minimum temperature drops.

In other work, and to complement the previous experiments,[3] another experimental EHD heat pipe has been tested with the results reported here. In this experiment a tent electromechanical flow structure was used to modify a conventional (feltmetal) capillary wick heat pipe. The purpose of this experiment was to determine whether an EHD flow structure would increase the maximum thermal throughput by shunting the high fluid resistance capillary flow path with the low resistance flow path of the tent structure. The experiments reported show that this kind of improvement is possible, though the over-all performance

as measured by the effective thermal conductance is not very good. The rather large temperature drops are thought to be due to the excessive thickness of the capillary wick lining the inside of the pipe.

Based upon the more recent experimental and theoretical findings, the conclusion has been reached that the most significant drawback of the electrohydrodynamic heat pipe is the required use of dielectric liquids as working fluids. Dielectric fluids suffer, when compared to more typical working fluids (water, ammonia), because of their poor thermal conductivity, low latent heat of vaporization, and low surface tension. Note that surface tension remains important in the EHD heat pipe designs promoted here, due to reliance upon capillary pumping for circumferential liquid distribution and collection.

The experiments conducted to date indicate that the electromechanical flow structures used have performed adequately, thus providing "proof of concept" for EHD heat pipes. The severe performance limitation in both experimental devices have been found to be in the capillary circumferential fluid distribution operation: (i) inadequate circumferential grooves in the first experiment[3] and (ii) grossly suboptimal feltmetal wicking in the second experiment*. Thus a need to consider the capillary flow and heat transfer problems for dielectric fluids has been well-eatablished. Present efforts in the project are directed at this issue.

*Chapter III of this report

II. THEORETICAL CONSIDERATIONS

A. DESCRIPTION OF GOALS

This section contains theoretical considerations for two basic problems. One is the prediction of the effective thermal conductance of an electrohydrodynamic heat pipe with threaded grooves for fluid distribution to the evaporator surface. An approximate result for the temperature drop at the evaporator is obtained by using known solutions for heat transfer in laminar flow through pipes and ducts. This result is applied to the geometry of the first heat pipe and effective thermal conductance is computed. In addition, the conductance calculation is applied to the flat-plate EHD heat pipe experiment.

The other problem considered theoretically is the design of threaded grooves for the evaporator of an electrohydrodynamic heat pipe. Solutions of relevant hydrodynamic equations are obtained. These solutions are investigated to determine conditions of optimum heat transfer at the evaporator. Design tradeoffs which allow more flexible heat pipe operation with respect to input heat and tilt are discussed. These calculations are applied to the flat-plate experiment to predict maximum heat input allowed before "burn-out" occurs.

B. APPROXIMATE HEAT PIPE CONDUCTANCE

Heat Transfer in Laminar Flow

The problem of heat transfer for fluid flowing in a capillary groove is similar to laminar flow through a pipe or duct. Several assumptions are made in calculating the amount of heat transferred in a duct.[4] Fully developed thermal and velocity profiles are assumed to exist throughout the length of the duct. Thus, entrance

region effects due to temperature and velocity changes are neglected for long tubes or ducts. In addition, the heat flow mechanism in laminar flow is purely due to conduction.[5] No mixing is assumed to exist in the fluid bulk. This allows heat conduction equations to be solved exactly for flow through a round tube and from this result, heat transfer in ducts of varying geometries is inferred.

To apply these calculations to capillary grooves in a heat pipe, the assumptions must be justified. In a capillary groove, laminar flow is assumed. This is well justified for the range of practical input heats in the heat pipe experiments. In addition, no thermal resistance is assumed to exist at the liquid surface where evaporation occurs. Hence, all thermal resistance is due to conduction through the liquid in the groove. In the case of entrance effects, velocity and temperature profile changes generally depend on the fluid Prandtl number. Velocity profile changes can be neglected if the tube length is approximately 50 times or more long wide.[5] This is consistent with the heat pipe groove dimensions. For liquids with a moderate Prandtl number such as Freon-113 (see Table I) the thermal profile develops at nearly the same rate as the velocity.[5] Consequently, entrance region effects for capillary grooves can be neglected.

Using these assumptions, the Nusselt number, Nu, has been plotted for various rectangular shapes.[6] The Nusselt number is a normalized measure of the effective thermal convection coefficient:

$$Nu = \frac{L\, h_c}{k} \tag{2.1}$$

where h_c is the convective heat transfer coefficient and L is an

NAME	SYMBOL	VALUE	MKS UNITS
Heat of Vaporization	λ	1.47×10^{5}	joules/kg
Dynamic Viscosity	μ	5.1×10^{-4}	kg/m-sec
Liquid Density	ρ_{ℓ}	1.5×10^{3}	kg/m^{3}
Dielectric Permittivity	ε	$2.33\varepsilon_{o}$	farads/meter
Surface Tension	σ	.019	newtons/meter
Thermal Conductivity	k	.066	watts/m-C°
Electrical Conductivity	σ_{ℓ}	$< 10^{-12}$	ohm^{-1}- $meters^{-1}$
Prandtl Number	Pr	7.1	dimensionless

Table I Properties of Freon-113

an appropriate length. In the case where groove dimensions are approximately equal, the Nusselt number for laminar flow is approximately equal to four.

Approximate Evaporator Conductance

To calculate the approximate thermal conductance of an evaporator, consider a flat-plate evaporator and condenser with rectangluar grooves cut into each end as shown in Figures 1a and 1b. Assuming that liquid is present in the evaporator grooves, the convection coefficient can be calculated by rearranging eq. (2.1):

$$h_c(x,z) = \frac{k\ Nu}{D_H(x,z)} \tag{2.2}$$

where k is the liquid thermal conductivity and D_H is the hydraulic diameter[4] associated with a particular fluid filled groove.

$$D_H = 4\left(\frac{\text{fluid cross-sectional area}}{\text{wetted perimeter}}\right). \tag{2.3}$$

The thermal conductance of an entire groove is then calculated by

$$G_{gr}(x) = 2w \int_0^{\ell_z} h_c(x,z)dz, \tag{2.4}$$

where w is the groove width and ℓ_z is the "wetted" length.
For an entire evaporator, the total thermal conductance is obtained by adding the thermal conductance of each groove.

$$G_{evap} = \sum_{i=1}^{n\ell_e} G_{gr}(i), \tag{2.5}$$

where n is the density of evaporator grooves, ℓ_e is the evaporator length, and $G_{gr}(i)$ is the thermal conductance of the ith groove.

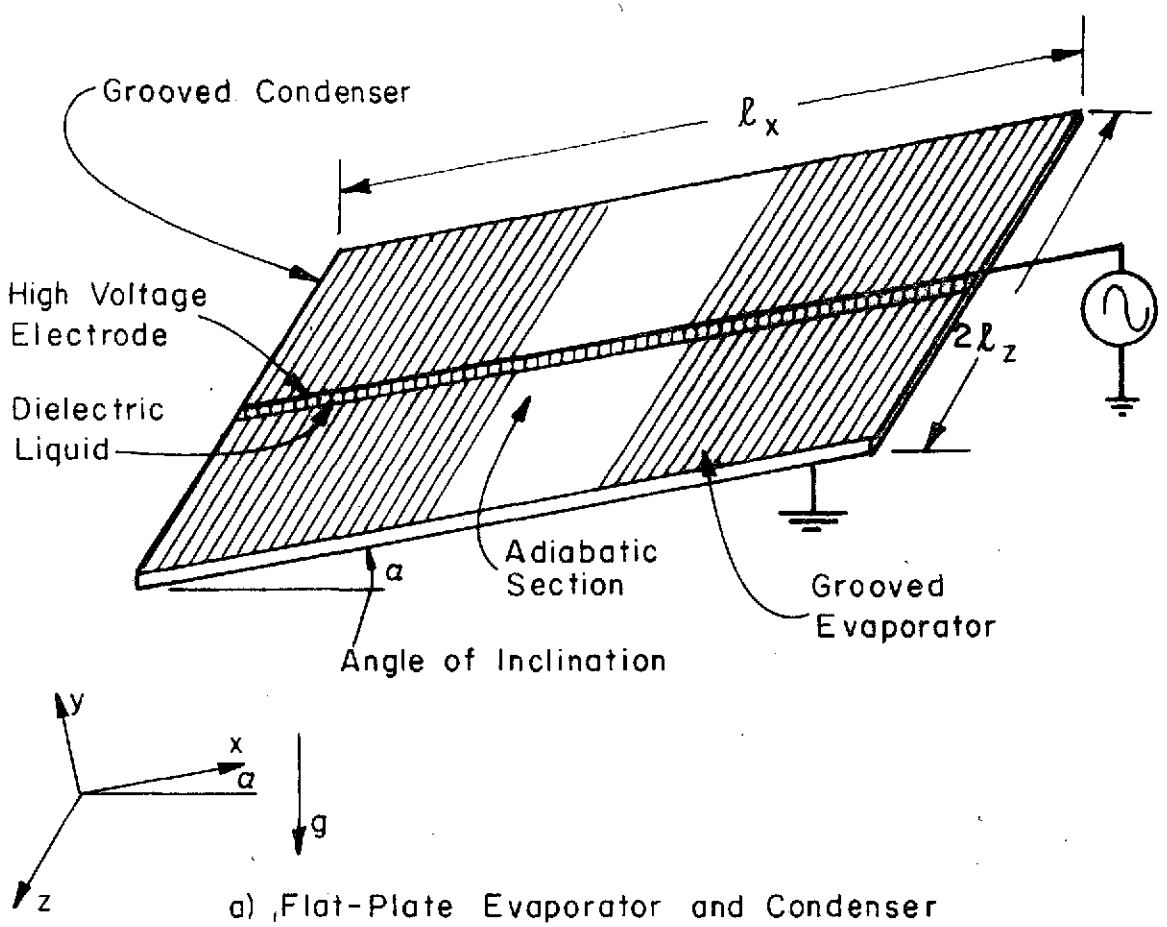

a) Flat-Plate Evaporator and Condenser Configuration.

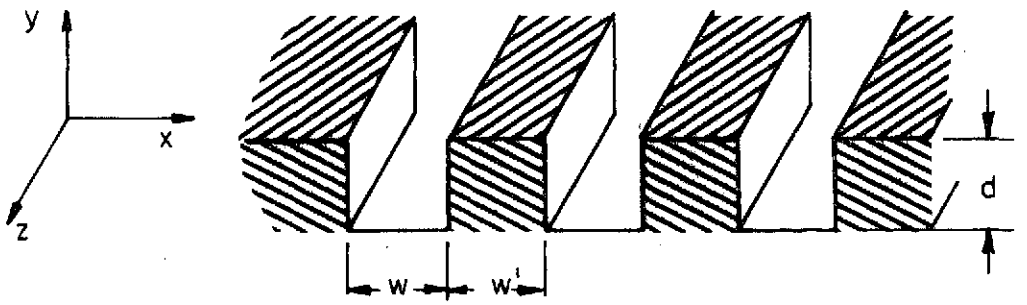

b.) Rectangular Groove Geometry in Flat-Plate Evaporator and Condenser

Figure 1

As an alternative to calculating the thermal conductance of an evaporator using eq. (2.5) further approximations can be used to make the calculation simpler. Assume that the convective heat transfer coefficient is constant over the evaporator surface. Let this quantity be calculated using the hydraulic diameter of a saturated groove, i.e.,

$$D_H = \frac{4wd}{w + 2d} . \tag{2.6}$$

Also, assume that thermal conductance is proportional to the entire evaporator area. Then, a rough approximation of the total thermal conductance can be made by

$$h_c \cong \frac{k\ Nu\ (w + 2d)}{4wd} \tag{2.7}$$

and

$$G_{evap} \cong \frac{k\ A_e\ Nu\ (w + 2d)}{4wd} . \tag{2.8}$$

where A_e is the total evaporator surface area. These approximations are reasonable since D_H is uniformly less than in eq. (2.6) for all grooves, while the area, A_e, is larger than the sum of all individual groove areas.

Other Contributions to Thermal Resistance

When evaluating the total heat pipe conductance, all significant factors contributing to temperature drops must be considered. In this treatment, no quantitative model is attempted for dynamic phenomena in the heat pipe other than evaporation. To get an approximate value of the thermal resistance between evaporator and condenser walls, temperature losses due to fluid in the vapor phase are neglected. A contribution to this effect could be caused by heat transfer from the vapor phase to the heat pipe walls in the adiabatic region.

Capillary threaded grooves are cut into the condenser section of the first experimental heat pipe and also the flat-plate heat pipe. This suggests that the condensation process could be similar to evaporation at the heated end. Laminar flow clearly develops in the capillary grooves at the condenser. Fluid is then pumped by the grooves and collected at the EHD artery. Hence, it may be inferred that the thermal resistance at an evaporator and condenser of equal areas will be nearly equal. The total heat pipe thermal resistance is thus roughly equal to twice the resistance at the evaporator surface.

Calculation of Heat Pipe Conductance

In this section, the results of the preceding analysis are used to get approximate conductance for the circumferentially grooved heat pipe and a proposed flat-plate heat pipe experiment. The Nusselt number in each case is assumed to be equal to four.

Table II gives the dimensions of the grooves in the cylindrical heat pipe tested. By experimental observation and direct calculation, the fluid pumping to the evaporator was found to be approximately 1 cm on each side of the artery. This observation was made under conditions of horizontal heat pipe orientation and no heat input. However, it is thought to be an accurate representation of the available pumping head due to the grooves with low heat input. Using the liquid thermal conductivity in Table I, the following results are obtained:

$$D_H = 2.6 \times 10^{-4} \text{m}$$

$$h_c = 10^3 \text{ watts/m}^2\text{-°C (evaporator)} \qquad (2.9)$$

$$G_{hp} = 2.3 \text{ watts/°C}$$

DESCRIPTION	SYMBOL	VALUE
Length of Heat Pipe	ℓ_x	.304 m
Length of Evaporator	ℓ_e	.114 m
Inner Radius of Evaporator	r_e	1.46×10^{-2} m
Area of Evaporator	A_e	.104 m^2
Width of Groove	w	2.9×10^{-4} m
Depth of Groove	d	1.2×10^{-4} m
Density of Grooves	n	2×10^{3} m^{-1}

Table II Dimensions of Grooved Heat Pipe

G_{hp} is the total heat pipe thermal conductance. This result is consistent with data from Research Report #3, in which heat pipe conductance varies between 2.5 watts/°C and 2.9 watts/°C at 25 watts input and 73°C condenser temperature.

Similar results can be obtained for the flat-plate device, assuming complete wetting of the evaporator surface. Measurements of groove dimensions were made of an aluminum plate obtained for experimental purposes. Table III shows approximate dimensions of this device. Calculations using the same formulae yield these results:

$$D_H = 4 \times 10^{-5} m$$
$$h_c = 6.6 \times 10^3 \text{ watts/m}^2\text{-°C} \qquad (2.10)$$
$$G_{hp} = 36.3 \text{ watts/°C.}$$

C. EVAPORATOR GROOVE DESIGN

Quantitative calculations can be made to investigate the performance for specific groove designs. This section contains the development of relevant hydrodynamic equations and approximate solutions for some cases.

Problem Definition

For simplification, the flat-plate heat pipe geometry is used in this analysis. The results obtained can be extended to other geometrical configurations. Figures 1a and 1b show the axes orientation with respect to the evaporator surface; $\hat{x}$ is along the axial flow structure and $\hat{z}$ points along a groove. The rectangular groove design shown in Figures 2a and 2b with dimensions (w,d) is considered.

DESCRIPTION	SYMBOL	VALUE
Length of Heat Pipe	ℓ_x	.304 m
Length of Evaporator	ℓ_e	.114 m
1/2 Width of Evaporator	ℓ_z	.05 m
Groove Width	w	1.9×10^{-4} m
Groove Depth	d	7×10^{-5} m
Density of Grooves	n	3×10^{3} m^{-1}
Area of Evaporator	A_e	1.1×10^{-1} m^2

Table III Dimensions of Flat-Plate Heat Pipe Experiment

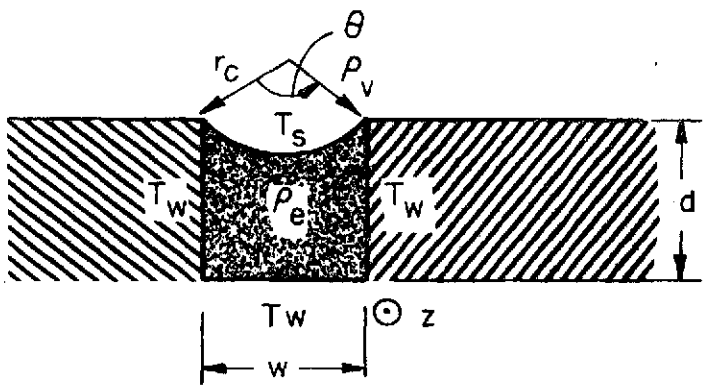

a) Fluid Configuration in a Groove

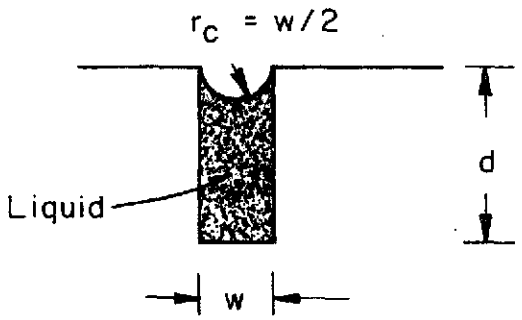

b) Deep Groove Case, w << d. Radius of Curvature of Liquid is w/2, the Maximum Curvature

Figure 2

Consistent with previous assumptions, uniform heat flux, q, is applied to the entire evaporator surface. Other parameters are then functions of spatial coordinates (x,z). At a given point in a groove, the wall temperature surrounding working fluid is constant. The liquid surface temperature is fixed over the entire evaporator. A list of symbols and definition of each is provided.

Hydrodynamic Equations

As a first quantitative relation, conservation of mass can be written for evaporation of fluid along a groove. The decrease in mass flow along the groove is proportional to the amount of evaporation due to input heat:

$$\frac{d}{dz}\left[A_x(z)\ u(z)\right] = -\frac{wq}{\rho\lambda} \tag{2.11}$$

Since the right side is independent of z, eq. (2.11) can be integrated directly. Differential equation (2.11) is ordinary since the grooves are hydrodynamically uncoupled from each other. The boundary condition in this case is that all fluid must be evaporated at $z = \ell_z$.

$$A_x\ (z)\ u(z) = \frac{wq}{\rho\lambda}\ (\ell_z - z). \tag{2.12}$$

An approximate relation for the steady fluid dynamics in the groove can also be written. The following result is obtained by differentiating Bernoulli's equation. Viscous loss along a groove is estimated by using the familiar hydraulic diameter concept of laminar flow through a tube.[7]

$$\frac{dp_\ell}{dz} = -\frac{32\mu u(z)}{D_H^{\,2}(z)} - \frac{1}{2}\rho u(z)\frac{du(z)}{dz}\ . \tag{2.13}$$

The pressure difference across a liquid vapor interface is known to depend on the surface radius of curvature r_c at that point.[8]

$$p_v - p_\ell = \frac{2\sigma}{r_c} \tag{2.14}$$

Differentiating eq. (2.14) with respect to z and assuming constant vapor pressure along z gives

$$\frac{dp_\ell}{dz} = \frac{2\sigma}{r_c^2(z)} \cdot \frac{dr_c}{dz} \tag{2.15}$$

Now, assume that kinetic energy loss is small compared to fluid pressure loss in eq. (2.13). This assumption is justified for the low fluid speeds typical of capillary grooves.[8] In addition, the liquid cross-sectional area can be uniquely computed from the radius of curvature,

$$A_x(z) = wd - r_c^2 \left[\frac{\theta}{2} + \frac{w}{2}\left[r_c^2 - \left(\frac{w}{2}\right)^2\right]^{\frac{1}{2}}\right] \tag{2.16}$$

where $\sin\frac{\theta}{2} = \frac{w}{2r_c}$. (2.17)

Using these results, a nonlinear, ordinary differential equation for r_c can be found.

$$\frac{\sigma}{\mu w_p^2}\left[\frac{A_x^3(z)}{r_c^2} \cdot \frac{dr_c}{dz}\right] = \frac{wq}{\rho\lambda}(z - \ell_z) \tag{2.18}$$

where w_p is the wetted perimenter,

$$w_p = w + 2d \text{ and } 0 \leq z \leq \ell_z \tag{2.19}$$

This equation can be solved to find the radius of curvature along a groove provided the boundary condition $r_c(z=0)$ is known.

Boundary Conditions

Notice that even though eq. (2.18) is ordinary, the unknown parameter, r_c, is a function of x and z. The boundary condition $r_c(z=0)$ depends on x, the groove location along the axial artery. To get this initial value, consider the liquid pressure variation inside the EHD flow structure, which is located at $z=0$.

$$p_\ell(x) = p_\ell(0) - \rho_\ell g x \sin\alpha - \Delta p_{x,visc} \tag{2.20}$$

where $p_\ell(0)$ is the liquid pressure at the surface of excess liquid at the condenser, and $\Delta p_{x,visc}$ is the hydrodynamic viscous loss along the axial artery. Other pressure losses are neglected. At the entrance of a groove, the radius of curvature depends on the liquid-vapor pressure difference across the meniscus.

$$p_v(x) - p_\ell(x) = \frac{2\sigma}{r_c(x,0)} \tag{2.21}$$

$p_v(x)$ is the vapor pressure at location x along the artery. At the condenser liquid surface $(x=0)$,

$$p_v(0) - p_\ell(0) = \frac{2\sigma}{r_c(0,0)} \tag{2.22}$$

Combining eqs. (2.21) and (2.22),

$$\Delta p_v(x) - \Delta p_\ell(x) = 2\sigma \left[\frac{1}{r_c(x,0)} - \frac{1}{r_c(0,0)}\right] \tag{2.23}$$

where $\Delta p = p(x) - p(0)$. If the condenser is operated in a saturated

condition, $r_c(0,0) = \infty$. In addition, the vapor pressure difference between evaporator and condenser is assumed to be negligible. Consequently,

$$p_\ell(0) - p_\ell(x) = \frac{2\sigma}{r_c(x,0)} \tag{2.24}$$

Plugging this equation into eq. (2.20), and assuming axial viscous losses are neglibible compared to gravitational pressure losses, the desired result is obtained.

$$r_c(x,\ z=0) = \frac{2\sigma}{\rho g x \sin\alpha} \tag{2.25}$$

Burn-Out Condition

The limiting condition on r_c for a given groove pertains to the maximum pumping ability of that groove. Clearly, for a groove which is deeper than it is wide, the minimum radius of curvature which the groove will support is one-half the groove width. Figure 2b shows this pumping limit concept. As the heat flux into a groove is increased, the radius of curvature at the end of the groove will decrease until the limit

$$r_c(x,\ell_z) = \frac{w}{2} \tag{2.26}$$

is reached. The groove then becomes burned out and pumping will cease prior to $z = \ell_z$, causing evaporative heat transfer to be drastically reduced. The maximum heat flux into a groove is reached when eq. (2.26) is satisfied. In a heat pipe, the evaporator groove farthest from the condenser will be the first to dry out as q is increased past the limit.

Solution to Hydrodynamic Equations

This section describes solutions obtained to the differential equation (2.18) subject to the boundary condition eq. (2.25) and the maximum pumping limit defined in eq. (2.26).

If eq. (2.18) is integrated between the limits of r_c imposed in the previous section the maximum value of heat flux input can be easily computed for a given rectangular groove of dimensions (w,d). Conversely, a desirable groove design can be determined if eq. (2.18) is integrated for a given q. However, a closed form solution is not possible for arbitrary grooves. A numerical solution is required to find the maximum possible heat flux input into the groove. Various values of q must be tried and eq. (2.18) integrated for each until the correct one is found. This iterative procedure is slow, expensive, and subject to computational round-off errors.

An approximate closed form solution to eq. (2.18) can be obtained for the case where groove depth is much greater than the width. Later, it is shown that this is a desirable, if hard to realize, condition. The liquid cross-sectional area is the difference between a "saturated" area and an area due to curvature:

$$A_x = A_o - A' \quad , \tag{2.27}$$

where $A_o = wd$, (2.28)

and $$A' = r_c^2 \cdot \sin^{-1}\left(\frac{w}{2r_c}\right) - \frac{w}{2}\left[r_c^2 - \left(\frac{w}{2}\right)^2\right]^{\frac{1}{2}} \tag{2.29}$$

In the case of $w \ll d$, $A' \ll A_o$ and

$$A_x^3 \cong A_o^2(A_o - 3A') \tag{2.30}$$

Plugging these equations into eq. (2.18), a simplified differential equation is obtained:

$$\frac{(wd)^2\sigma}{\mu(w+2d)^2}\left[\frac{wd}{r_c^2} - 3\sin^{-1}\left(\frac{w}{2r_c}\right) + \frac{3w^2\sqrt{\left(\frac{2r_c}{w}\right)^2 - 1}}{2r_c^2}\right]\frac{dr_c}{dz} = \frac{wq(z-\ell_z)}{\rho\lambda} \tag{2.31}$$

Eq. (2.31) is easily integrated between the desired limits to produce the following expression:

$$\frac{\sigma(wd)^2}{\mu(w+2d)^2}\left[2d + \frac{3\pi w}{4} - \frac{wd}{r_o} - 3r_o\sin^{-1}\left(\frac{w}{2r_o}\right) - \frac{3w^2}{4r_o}\sqrt{\left(\frac{2r_o}{w}\right)^2 - 1}\right] = \frac{wq\ell_z^2}{2\rho\lambda}, \tag{2.32}$$

where q is now the maximum allowed input heat flux and $r_o = r_c(x,z=0)$.

Plots of maximum heat flux versus w are found in Figures 3a, 3b and 3c. Note that only portions of the complete curves have been obtained, since the condition $w<<d$ is imposed. The points marked by dots on the curves denote numerical trial and error solutions of eq. (2.18). The various graphs represent different values of the groove depth. On each graph are three plots corresponding to different initial conditions on r_c. The smallest initial value is obtained using x equal to the length of the flat heat pipe, $\alpha=10°$, and fluid properties of Freon-113. Other values of r_o used are twice this amount, and r_o = 1 m.

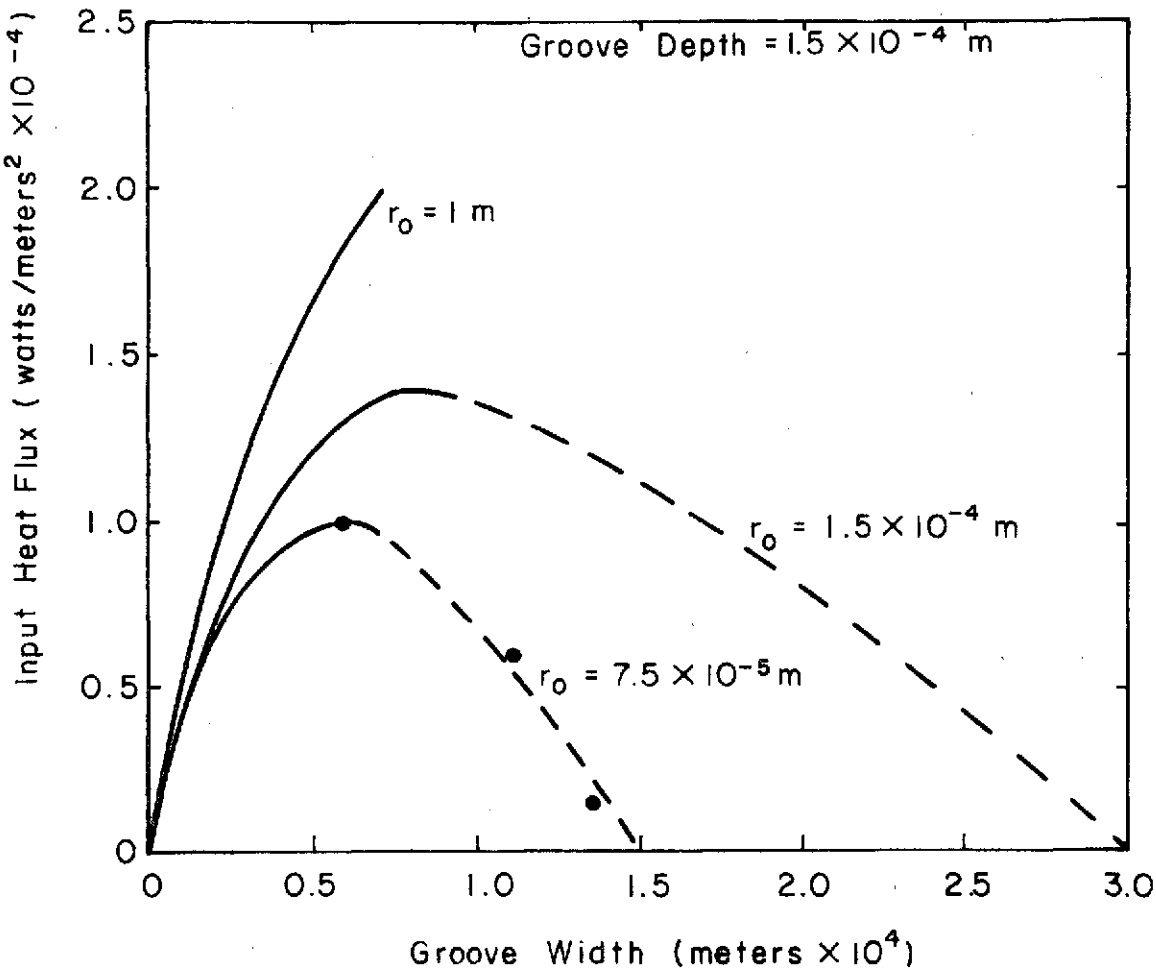

Figure 3a) Maximum Heat Flux vs. Groove Width

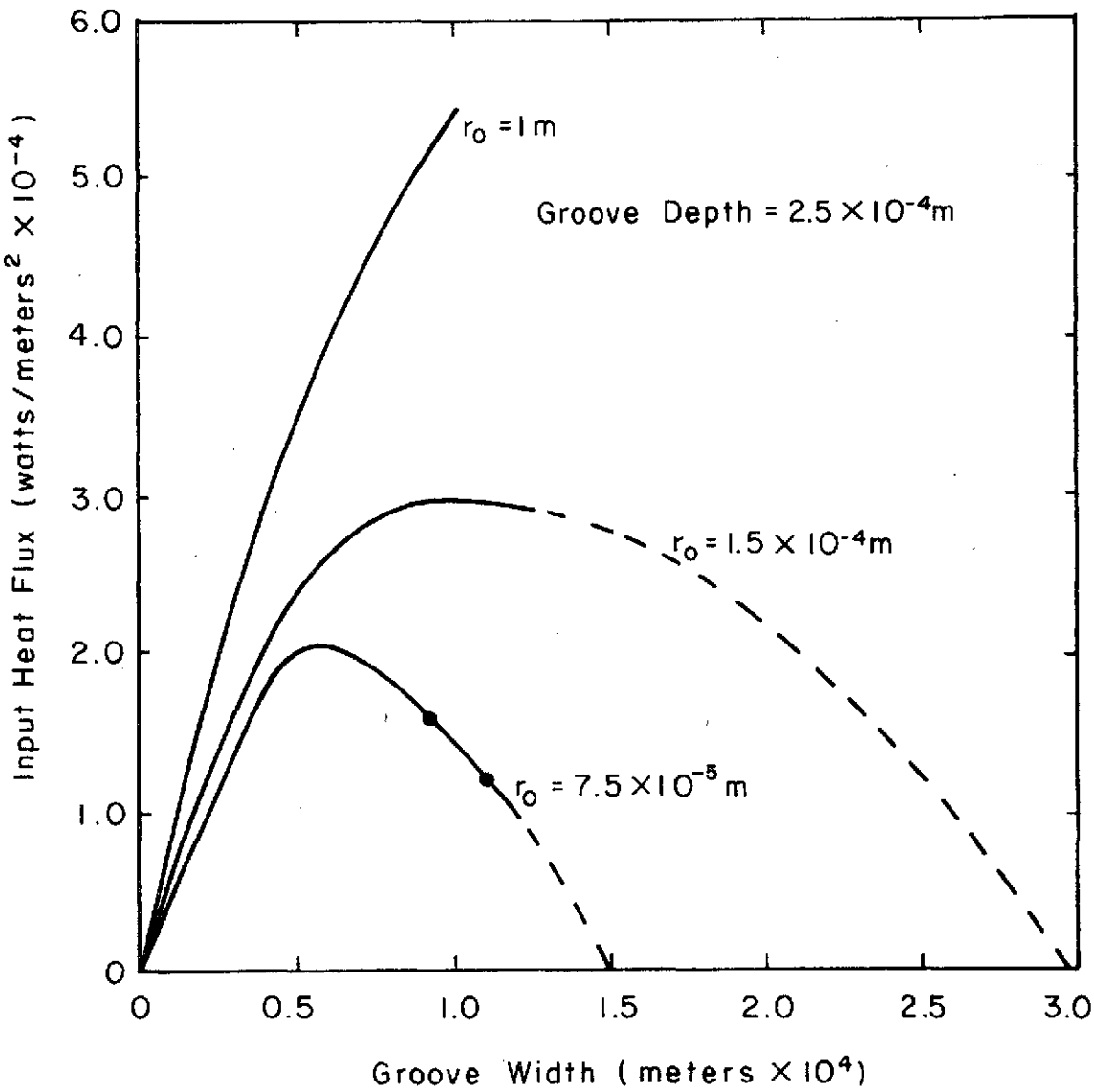

Figure 3b) Maximum Heat Flux vs. Groove Width

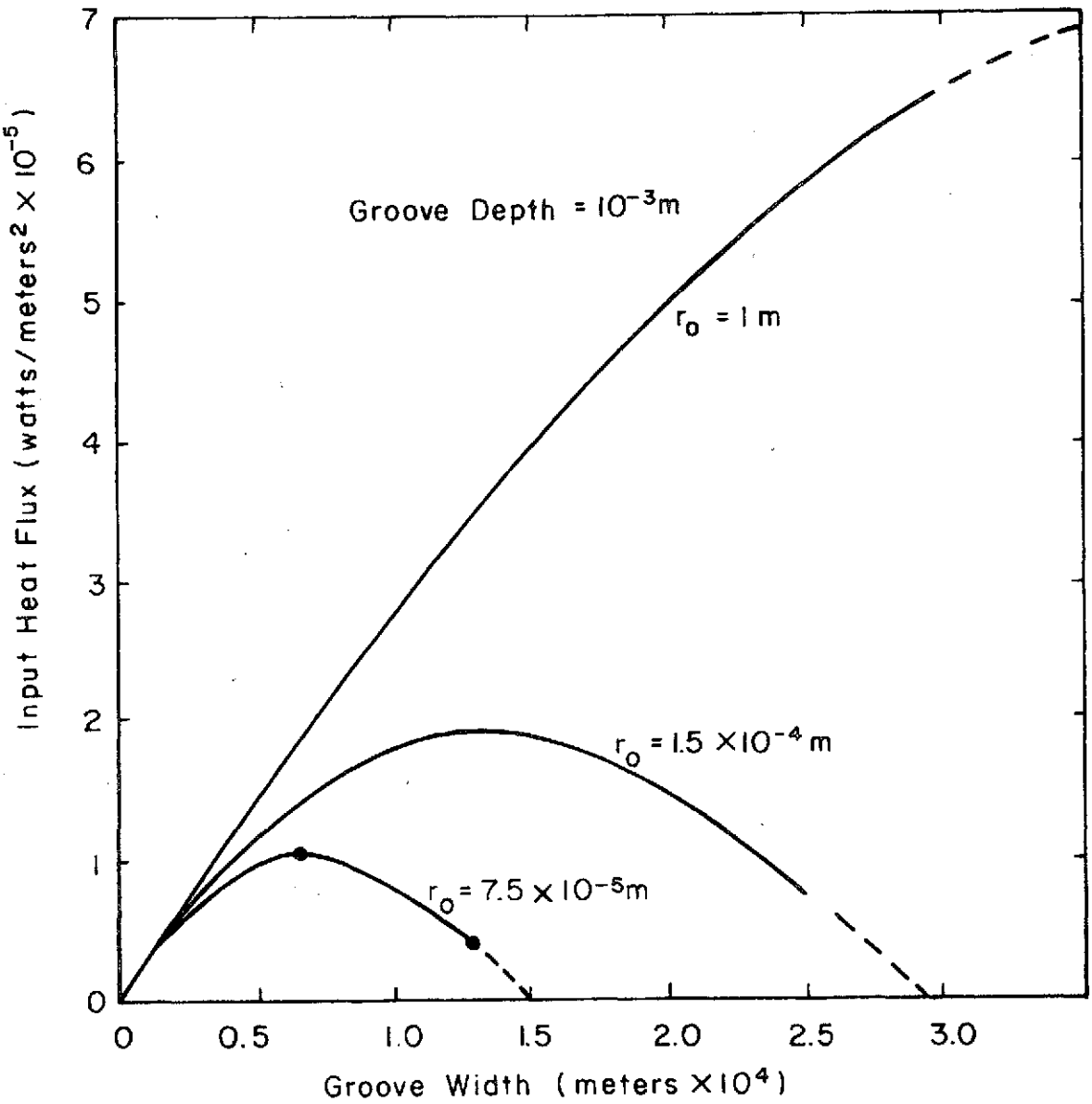

Figure 3c: Maximum Heat Flux vs. Groove Width

Comments on Maximum Heat Flux into a Groove

The plots in Figure 3 all show similar characteristics. At $w=0$ and $w = 2r_c(x,0)$, no heat is transferred by evaporation. For $w = 2r_c(x,0)$, no capillary pumping is obtained from the grooves, so the evaporator groove remains essentially unwetted. At some point between the two extremes, a maximum heat flux exists. The maximum heat flux increases with larger initial radius of curvature and increased groove depth, since these conditions allow greater flow capacity in the groove. This suggests that the maximum possible groove depth is desirable in heat pipe fabrication.

Two basic forces are affecting the curves obtained for maximum heat flux. As w approaches zero, viscous forces begin to appear and eventually dominate the hydrodynamics. Maximum heat input is reduced since capillary pumping cannot overcome viscous losses. As w increases, the capillary pressure head available for liquid pumping is reduced. This tends to decrease the maximum possible heat flux. The combination of these two phenomena causes heat flux curves to pass through a maximum with respect to w.

D. DISCUSSION OF THEORETICAL RESULTS

Heat Pipe Conductance and Groove Design

To summarize results obtained in previous sections, groove design and heat pipe performance are discussed in this section.

The ultimate goal in heat pipe design is that sufficient overall thermal conductance between evaporator and condenser be achieved. The temperature drop as a function of spatial coordinates for a grooved evaporator is thus desired. As an approximation, assume that the temperature difference is proportional to the hydraulic diameter, i.e.,

$$\Delta T(x,z) = \frac{q\ D_H(x,z)}{4k} \quad . \tag{2.33}$$

This is a reasonable approximation for several reasons. First, as is easily shown, this corresponds to a constant Nusselt number of four. This result is employed in Section B of this chapter to predict the approximate performance of a threaded groove heat pipe. Further, ΔT is a monotonically increasing function as w approaches d for fixed d. Hence, groove conductance increases as the width decreases. This is an expected result. Notice that $\Delta T(x,z)$ is minimized near $z = \pm \ell_z$ at conditions approaching burn-out. The outer extremity of the last evaporator groove is the point where the smallest temperature drop occurs.

Now consider this temperature drop approximation and a typical heat flux curve in Figure 3. If a specific heat flux is desired, the groove depth and initial radius of curvature for the last evaporator groove must be sufficiently large. In general, a range of groove widths are then available which will allow the specified input level. The smallest width achieves maximum conductance but allows no flexibility for increasing heat input or increasing heat pipe tilt. The largest width achieves poorest conductance but also allows no flexibility in input conditions. To design for a situation in which operating conditions could be changed without burn-out, an intermediate width w might be chosen. Maximum flexibility would be obtained by choosing w to be the value corresponding to the q_{max} peak.

Extension of Theoretical Results

The results of analysis present in Section C of this chapter for a flat evaporator with rectangular grooves can be generalized to include other configurations.

If the evaporator is not flat, eq. (2.13) can be modified to include the pressure gradient due to gravitational body force along the groove. For the cylindrical heat pipe geometry employed in the experiment, this modification could be used to investigate groove requirements.

In addition, non-rectangular groove designs can be used in the theoretical model. Specifically, triangular and circular grooves have been proposed as desirable pumping mechanisms.[9] Triangular grooves seem to be attractive for evaporation since the average liquid film thickness would tend to be smaller.

The modification required for other groove geometries is simple. The hydraulic diameter defined in eq. (2.2) can be applied to any desired groove geometry. Figures 4a and 4b show these other two groove designs. Changes in hydraulic diameter would effect viscous losses for hydrodynamic equations and also the temperature drop for a given input heat. Hence, solution of eq. (2.18) can be obtained for a desired groove geometry in a manner identical to the method used in Section C for rectangular grooves.

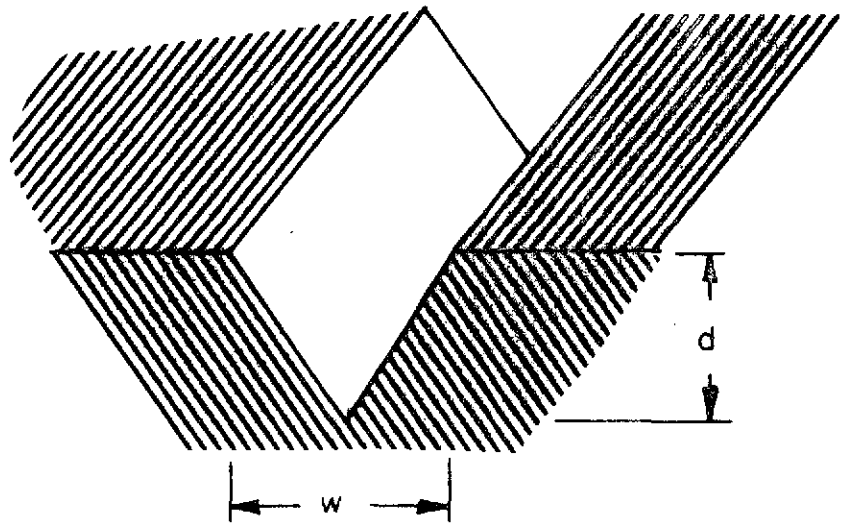

a) Triangular Groove Configuration.

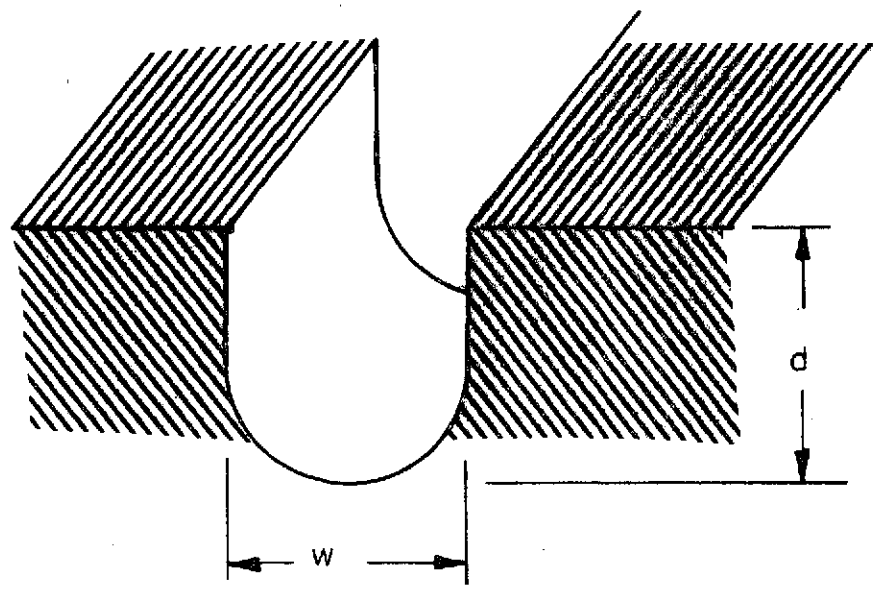

b) Possible Cylindrical Groove Configuration.

Figure 4

III. CAPILLARY FELTMETAL EHD HEAT PIPE EXPERIMENT

This section describes the second experimental heat pipe in which an EHD flow structure is employed. This device is characterized by the presence of an axially mounted electrode to provide EHD pumping from condenser to evaporator. Figures 5a and 5b show the physical configuration of this experiment. The heat pipe has capillary wicking material for conventional operation. The wicking material provides distribution of fluid to the entire evaporator, as well as axial fluid pumping. Viscous losses along an EHD artery are thought to be negligible compared to those in a typical capillary wick. Hence, it was hoped that the EHD flow structure would shunt the axial flow resistance due to the porous capillary wick. In this experiment, heat pipe performance is not limited by poor fluid pumping in circumferential grooves, as has been observed in the first. The entire evaporator area is supplied with liquid in this case.

A conventional feltmetal capillary heat pipe was obtained. This heat pipe consists of a 15.3 cm length of 2.5 cm OD stainless steel pipe with .16 cm wall thickness. The inner walls are lined with a .16 cm layer of copper feltmetal, attached by silver solder. The feltmetal lining is intended to provide axial and circumferential fluid pumping for conventional heat pipe operation.

This heat pipe is modified by the placement of a wire electrode mounted axially inside the pipe approximately 0.3 cm above the feltmetal surface. Plexiglas ports are fitted on each end so the wire electrode can be mounted easily and insulated from the conducting walls. The heat pipe is sealed using a low vapor pressure epoxy resin. In a manner similar to the first experiment,[3] a water jacket is placed

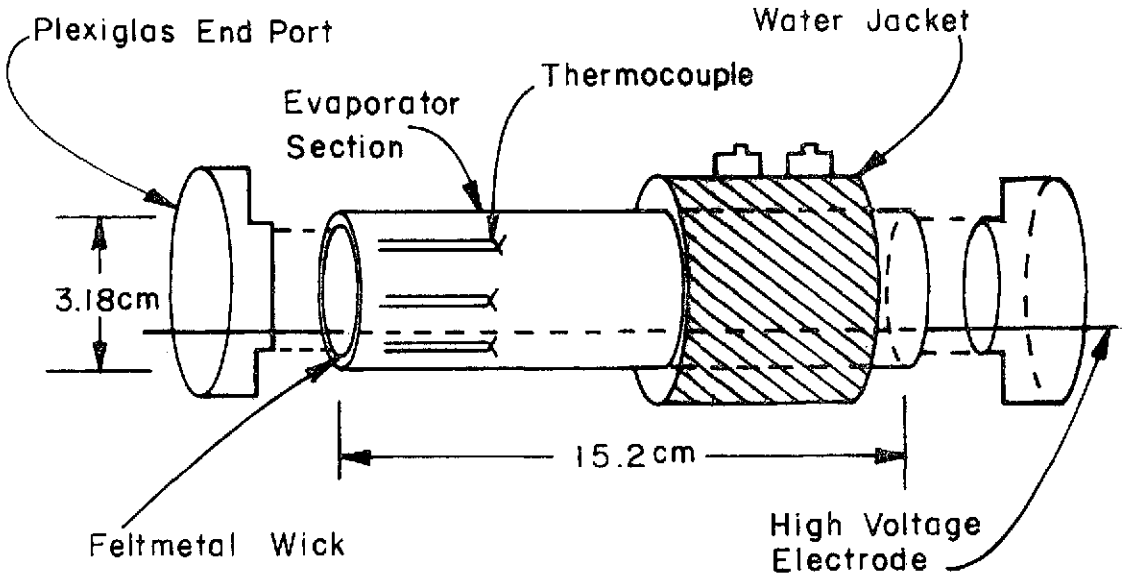

a) Exploded View of Feltmetal Heat Pipe

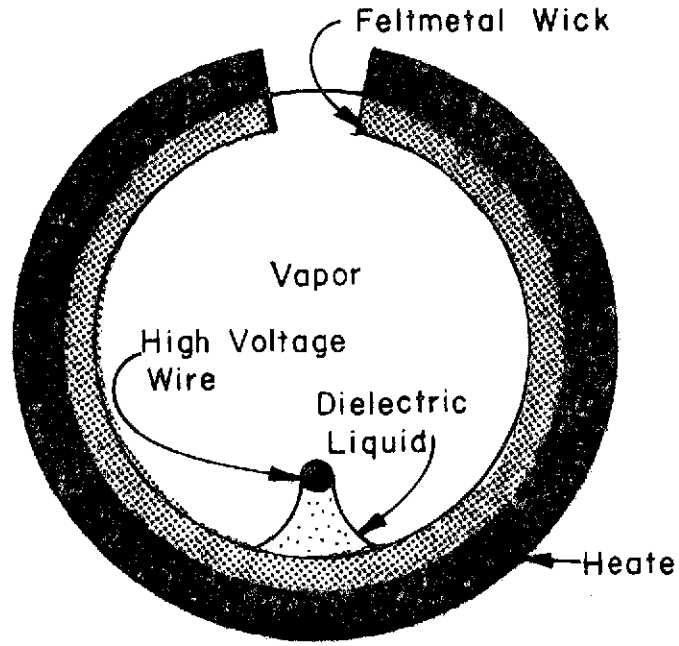

b.) Cross-sectional View of Second Electrohydrodynamic Heat Pipe Experiment with Feltmetal Capillary Wick and Tent Electromechanical Flow Structure

Figure 5

over the condenser and thermocouples are fixed to evaporator walls and placed in the water jacket. The evaporator and condenser sections are approximately 6.4 cm long, separated by a 2.5 cm adiabatic section. A heater is designed to heat uniformly the entire evaporator surface. A spatially varying electrode is employed and Freon-113 is used as the working fluid. The heat pipe cavity is evacuated to about .03 mm Hg prior to introduction of the fluid.

Thermocouple locations on the evaporator walls are shown in Figure 5a. A total of six thermocouples are fixed at approximately equal intervals around the evaporator. Due to the short evaporator length, no more than one thermocouple is placed in line along the heated area. Additional thermocouples are mounted outside the heater and insulation to monitor any input heat losses.

C. PROCEDURES

Experimental Procedure

The experimental techniques for obtaining data from the second EHD heat pipe experiment are described in this section. Prior to the initiation of an experiment, heaters are fixed to the evaporator walls and well-insulated from the outer environment to minimize losses. With the heat pipe cavity fully evacuated, the vacuum valve is closed and working fluid is introduced at room temperature from a graduated burret. Sufficient fluid is introduced so that a small excess forms at the bottom. This excess fluid provides an axial pumping mechanism for horizontal heat pipe operation. When the evaporator is raised above the condenser, the excess fluid fills the electrode flow structure when voltage is applied. The working fluid used in all heat pipe experiments

is Freon-113. Table I lists the properties of this fluid. The fluid inventory in each heat pipe is varied to some extent, but no perceptible change in heat pipe performance is observed.

To begin an experiment, heat is applied to the evaporator section and the condenser temperature is established. After allowing thermal equilibrium to be reached with the heat pipe horizontal and no voltage, a measurement of thermocouple voltages is made. When voltage is applied with the heat pipe still horizontal, no effect on thermocouple temperatures is observed. Further measurements are made by lifting the evaporator above the condenser, and applying sufficient voltage to the electrode such that the fluid fills the entire electrode length. Approximately 25 minutes are allowed for temperature transients to disappear between measurements. The evaporator is lifted above the condenser until electrical breakdown in the vessel occurs. The basic procedure for testing a heat pipe consists of measuring thermocouple voltages for various tilts and sufficient voltage to allow operation.

When possible, measurements are made on evaporator thermocouples at each tilt with no voltage applied to the electrodes. This is done to compare heat pipe operation with and without EHD pumping between condenser and evaporator. This procedure is particularly meaningful in the second heat pipe, in which capillary material provides some pumping for returning liquid, since this allows the direct comparison of capillary and EHD flow structure efficiency. Unfortunately, these comparisons are limited at high thermal throughputs by high temperatures which develop at zero voltage when the evaporator is dry. To avoid damage to thermocouples and other materials, this procedure is terminated when excessively high temperatures are reached.

In addition, measurements are taken of thermocouple voltages with no fluid in the heat pipe for both devices. This is done so that axial thermal conductance through the heat pipe walls can be computed. The effective conductance of the walls is also verified by direct calculation.

In this experiment, approximately 9 ml of fluid is needed before any excess accumulates on the bottom. Another 3 ml is introduced in order to provide the required excess. This brings total fluid inventory to approximately 12 ml. This amount is not varied significantly from one test to another. It is verified by observation that the entire feltmetal lining is wetted by fluid under these conditions. On a volume basis this amount is a huge increase in fluid inventory over the first experiment[3] (where the heat pipe cavity volume is approximately four times as large as the feltmetal device).

Experimental procedure is similar to that for the first experiment. Higher tilts are obtained for the second experiment due probably to closer electrode spacing. Results from this experiment are plotted in Figures 6a and 6b. Again, the temperature drops from evaporator to condenser are insensitive to tilt. With no voltage applied, the temperature difference increases rapidly as tilt is increased, despite axial capillary pumping. This is proof that the EHD artery does a better job of axial pumping than the feltmetal. Note the temperature curves for input heat of 20 watts in Figures 6a and 6b. Results show the voltage has no effect on heat pipe performance for any tilt. This indicates that evaporator burn-out occurs between 20 and 40 watts input. Subsequently, tests were made to determine where burn-out occurs with no voltage.

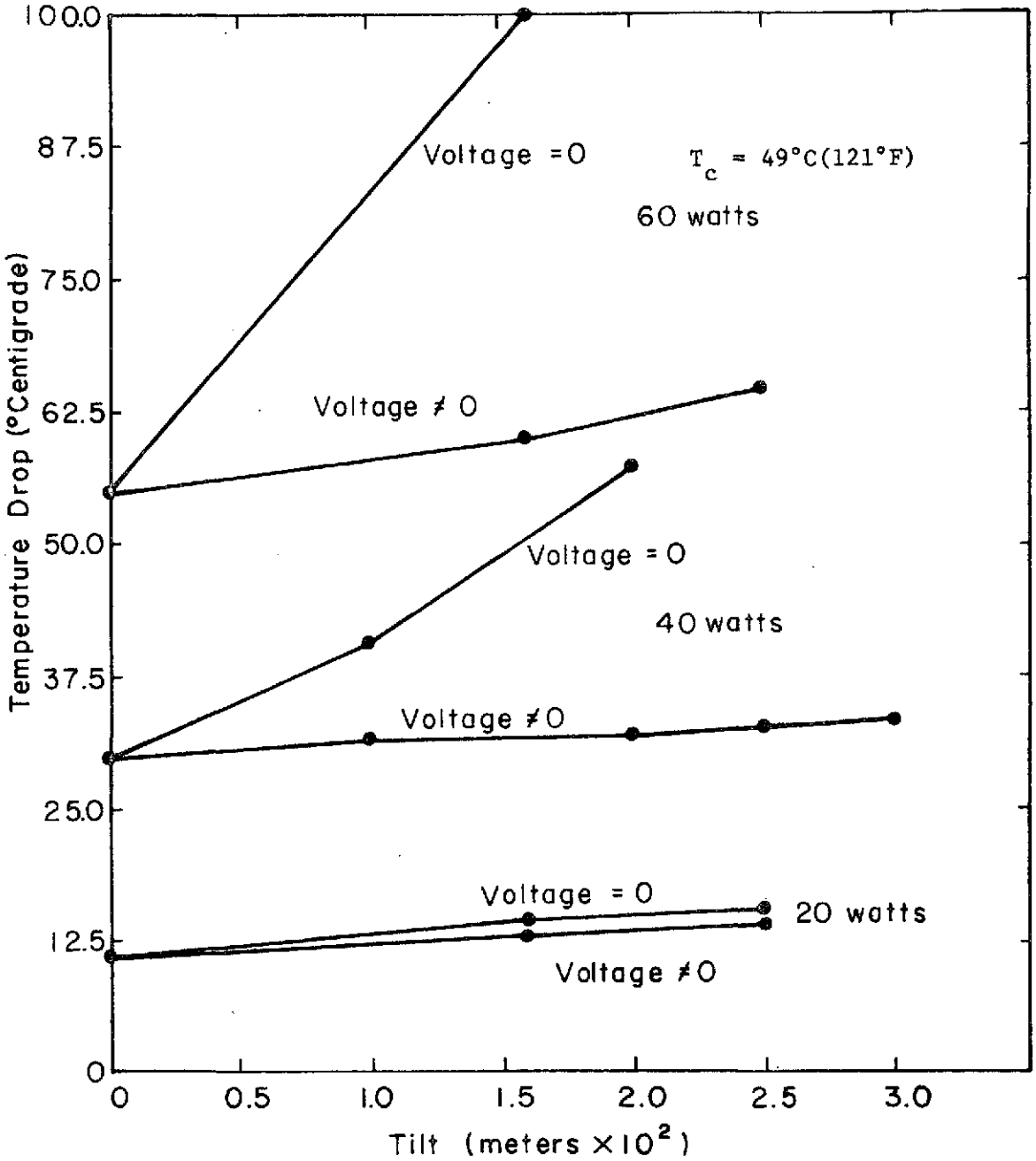

Figure 6a) Evaporator-Condenser Temperature vs. Tilt for Feltmetal EHD Heat Pipe

Condenser Temperature = 49°C

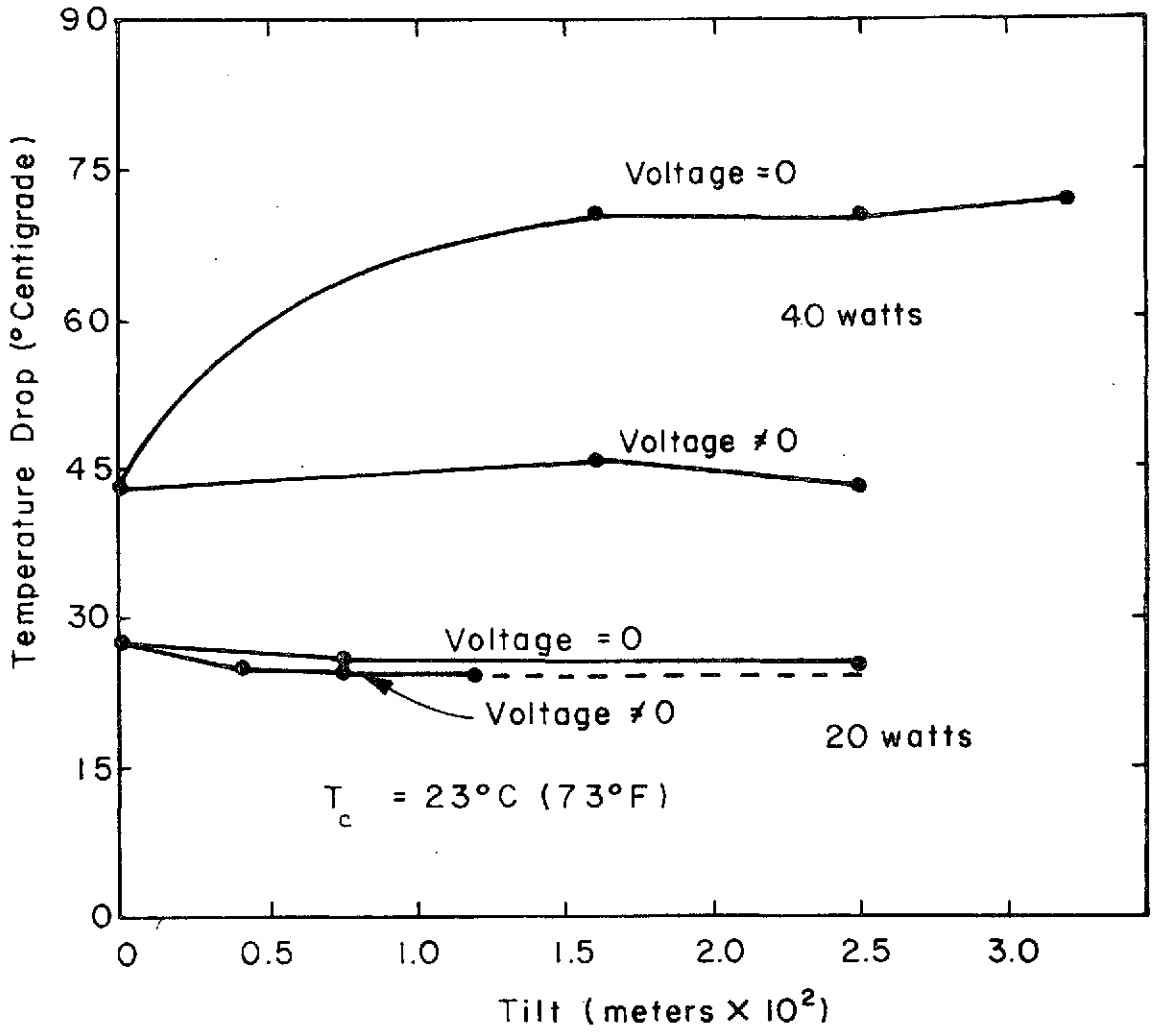

Figure 6b) Evaporator-Condenser Temperature vs. Tilt for Feltmetal EHD Heat Pipe
Condenser Temperature = 23°C

Figure 7 shows the results obtained with the feltmetal wick just saturated with liquid and with no excess on the bottom. For the tilts considered, heat pipe conductance falls off dramatically between 20 and 25 watts, while falling off more slowly afterwards. Hence, it is assumed that the evaporator starts to burn out between 20 and 25 watts for both tilts. Notice that conductance is better for lesser tilts as expected. With excess fluid at the bottom and no tilt, the heat pipe conductance is constant since the axial flow resistance is shunted by excess inventory. However, when the evaporator is raised, the excess fluid collects at the condenser end. Unless voltage is applied to establish axial flow, the heat pipe is dependent on axial capillary pumping to return the fluid.

When considering the data with respect to overall heat pipe conductance, it is clear the feltmetal EHD heat pipe is a poor heat conductor. This is undoubtedly due to thermal blanketing of the vapor from the evaporator walls by the thick layer of dielectric fluid in the wick. Since the evaporator feltmetal is saturated by Freon-113 working fluid, a layer of insulating fluid is causing larger thermal resistance to the input heat. Overall heat pipe conductance is even worse than in the first experiment,[3] despite the shorter length of the second device. This experiment demonstrates the characteristic that dielectric liquids with low electrical conductivity tend to insulate thermally the evaporator walls because of their low thermal conductivity.

Execution of this experiment is hampered because of pressure leaks which develop at high temperatures. Since "O" rings are not used to seal the end ports, the pressure seal is maintained by low vapor

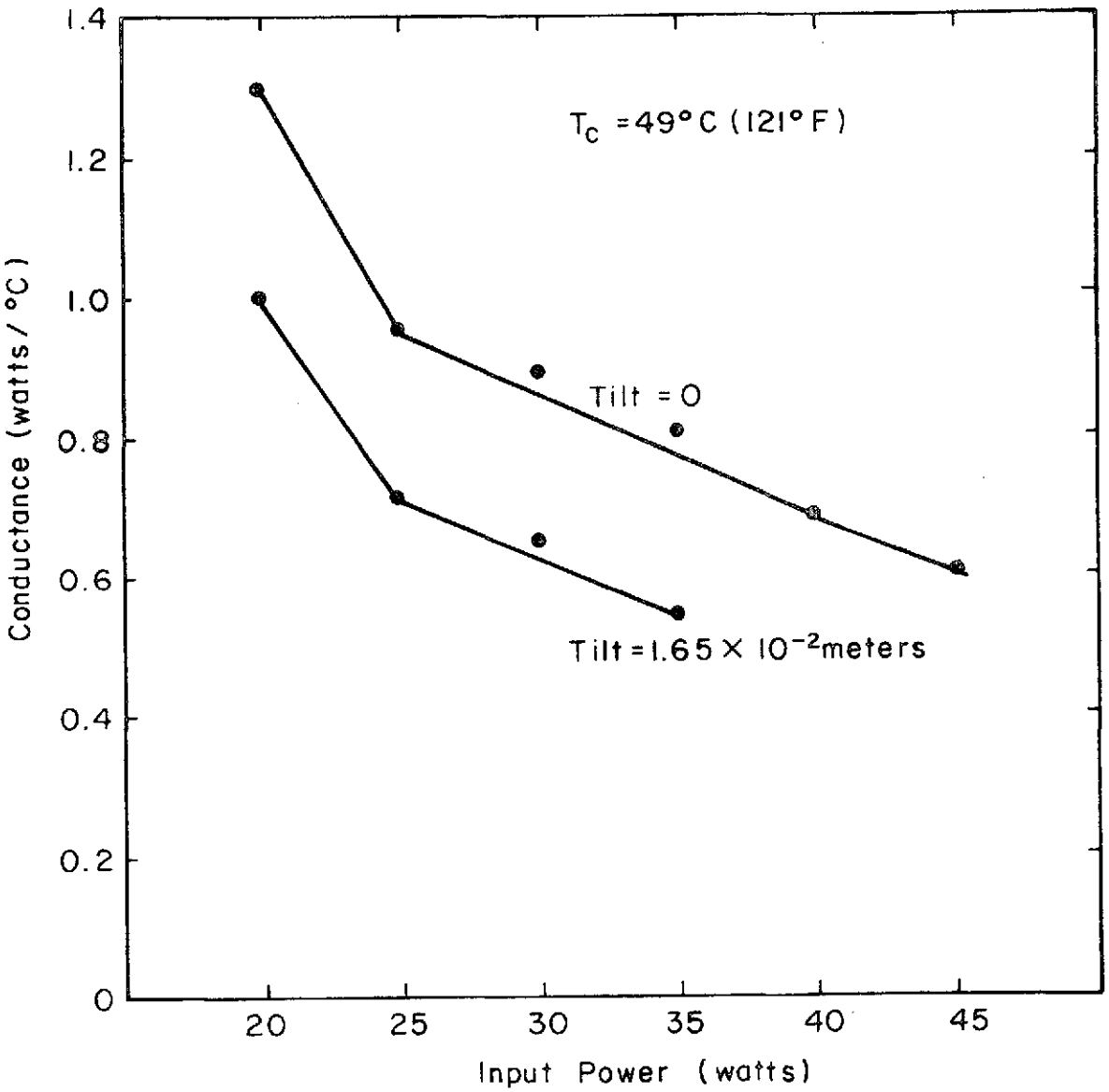

Figure 7 Feltmetal Heat Pipe conductance vs. Input Power when Capillary Wick is just Saturated with Liquid and No Voltage Applied

pressure epoxy. Above a certain temperature, the epoxy cracks and leaks develop. This puts a limitation on the condenser operating temperature. In this experiment, no tests are made with the condenser temperature at 73°C, and the burn-out curves in Figure 6 are not completed. However, the data trend is well-established despite this restriction.

Each time a leak develops, the heat pipe is disassembled and a new electrode is mounted for the next experiment. This means that the electrode is usually free of defects which cause fluid surface instabilities. Hence, dc high voltage is used exclusively in this experiment, and no fluid surface disruptions are encountered.

At the beginning stages of this experiment, a short circuit was induced several times when voltages above 10 kv were applied. It is conjectured that the short was caused by feltmetal being pulled from the inside walls by strong forces which are present between the electrode and the feltmetal surface when high voltage is applied. The problem was encountered only in the early stages of experimentation, suggesting that all "loose" feltmetal was eventually pulled up and removed during cleaning. However, this phenomenon could pose a question as to the compatibility of feltmetal wicks and electromechanical flow structures.

The long term effect of F-113 fluid in a feltmetal wick has not been determined. However, the heat pipe was soaked for several days in the working fluid to eliminate impurities which appeared in the fluid when first introduced into the cavity.

IV. DISCUSSION

A. CONCLUSIONS BASED ON THEORETICAL RESULTS

Theoretical considerations have been directed at two primary objectives. A simple model for estimating thermal conductance of a grooved heat pipe is derived. In addition, a hydrodynamic model for liquid flow in a capillary groove is presented. Approximate solutions to these equations are obtained. The solutions provide a quantitative method by which evaporator grooves in a heat pipe can be designed.

The model for approximate thermal conductance of a grooved heat pipe is based on known solutions for heat transfer in laminar flow through a duct. For long tubes and ducts, a constant Nusselt number of four is assumed along the entire length. This result gives an effective convection coefficient which depends on the variable hydraulic diameter. A rough calculation is made assuming constant hydraulic diameter and letting the entire evaporator area contribute to evaporation. The estimated conductance for the grooved heat pipe is close to the experimental result obtained at 25 watts input, and 73°C operating temperature. However, the theoretical model does not take into account changes in condenser temperature or variations of input power.

The problem of evaporator groove design to achieve optimal heat pipe performance is also discussed. Solutions to hydrodynamic differential equations give curves which show the maximum amount of input heat the groove can accept before burn-out occurs. Basic factors which control performance of a rectangular groove are its width and depth, as well as liquid curvature at the entrance to the groove. Maximum pumping ability of a groove occurs when the liquid radius of curvature

equals one half of the groove width. The initial radius of curvature is dependent on the heat pipe tilt in a gravitational field.

Investigation of the theoretical curves produces the following conclusions. Under any conditions, the maximum groove depth obtainable is desired. Groove depth fixes the quantity of liquid present in a groove. Therefore, more liquid can be evaporated when groove depth is increased. As expected, greater tilt of the heat pipe produces a smaller radius of curvature at the groove entrance. Hence, greater tilt causes decreased flow capacity and resulting evaporation limitations. Increased groove depth reduces this effect.

For design purposes, groove width is the critical parameter. Increased pumping by narrower grooves is counteracted by increased losses due to viscous forces. For a given heat input, groove depth, and initial radius of curvature, a range of groove widths exists which allows the entire groove to be wetted. The smallest of these widths will yield the smallest temperature drop. At this point, increased heat input will cause burn-out to occur because of viscous forces. Hence, a slightly greater groove width might be desired to allow some flexibility in heat input.

These results can be extended easily to include other cross-sectional groove geometries.

B. EXPERIMENTAL RESULTS

Most conclusions reached about the EHD heat pipe described in Chapter III of this report are essentially consistent with those communicated earlier regarding the first experimental device.[3] Once again an electromechanical flow structure has been successfully used for axial

liquid transport in a heat pipe. The structure serves as an artery for the fluid which is pumped from the condenser to the evaporator surface. However, unlike the first experiment, axial pumping by both capillarity and EHD polarization forces is possible in this device, This second experiment is significant because viscous losses along the EHD flow structure are shown to be negligible compared to the flow resistance due to the feltmetal material.

Experiments show again that the variable conductance feature for EHD heat pipes is a built-in capability for terrestrial applications. If the heat pipe is slightly tilted, the voltage source becomes the mechanism by which the heat pipe can be turned on and off. Similarly, by continuously varying the voltage under these conditions, total heat pipe conductance can be varied between nearly zero and 100% of its maximum value. Hence, the high voltage source becomes the controller of heat pipe conductance.

Plots of experimental data show that uniform thermal conductance is achieved over a range of tilts. The experiment also provides a comparison to conventional heat pipe operation in regard to this property. When the EHD flow structure is not used, capillary forces are relied upon to provide axial pumping. Heat pipe conductance then falls off rapidly as tilt is increased.

Heat Pipe Thermal Conductance

Overall thermal conductance of the second experimental heat pipe is once again also very poor. The thick layer of feltmetal lining the inside heat pipe walls fills with dielectric fluid. The resulting liquid layer thermally insulates the hot evaporator walls from the fluid surface where evaporation takes place. Evidently, conduction of

heat to the liquid surface by the feltmetal fibers is not significant enough to reduce this effect.

Other Experimental Results

The compatibility of EHD flow structures and capillary grooves was established in the first experiment.[3] In the second experiment, some difficulty was encountered as short circuits between electrodes developed when high voltage was applied. However, as the experiment progressed, this phenomenon diminished. It is thought that electrical forces pulled loose feltmetal from the capillary wick, causing the short circuit. Hence, the compatibility of feltmetal capillary wicks and EHD flow structures is subject to question.

C. FURTHER GENERAL DISCUSSION

Both electrohydrodynamic heat pipes tested thus far have exhibited a similar set of characteristics. Certainly, the concept of using an electromechanical flow structure for axial liquid flow from condenser to evaporator is proven out at this point. On the other hand, the performance has not been highly encouraging primarily based on experimental thermal conductance values. The experience gained with these devices has indicated a striking mismatch of the EHD forces utilized for axial flow and the capillary forces relied upon for circumferential distribution and collection. Further, poor condensation and evaporation heat transfer coefficients have been encountered. Both of these problems stem from the generally poor capillary fluid transport factors of the organic and fluorocarbon dielectrics used in EHD heat pipes. Any heat pipe using these liquids as working fluids thus suffers from the obvious disadvantages that low thermal conductivity, surface tension, and latent

heat of vaporization bring. Still, the plausible future requirement of a heat pipe operating in the range of utility of the dielectric liquids (250°F to 750°F) would seem to justify efforts to determine the ultimate capability of electrohydrodynamic heat pipes. This statement is reasonable because it has been shown (for at least one case) that an electromechanical flow structure can greatly enhance the performance of a conventional heat pipe using a dielectric working fluid.*

The inescapable conclusion is that effort should be directed at the design and construction of an EHD heat pipe device where sufficient attention has been given to the design of an adequate capillary distribution network of circumferential grooves, or wicking material. Previous performance estimates[1,10] were misleading because this part of the problem was not recognized in the early stages of the research. With the theory and optimization techniques developed by Perry[11] and reviewed here, much more reliable performance calculations should be possible for electrohydrodynamic heat pipes.

* Refer to Fig. 6a, b of this research report.

ACKNOWLEDGEMENT

The authors are indebted to A. Basiulis of Hughes Aircraft Company, Torrance, California, who provided the feltmetal heat pipe used in the experiments reported in Chapter III.

APPENDIX

NOMENCLATURE

A_e	evaporator surface area
A'	liquid cross-sectional area correction due to curvature
A_o	cross-sectional area of a groove
A_x	liquid cross-sectional area in a groove
D_H	hydraulic diameter of a groove containing fluid
G_{evap}	total thermal conductance of evaporator
G_{gr}	thermal conductance of a groove
G_{hp}	heat pipe thermal conductance
L	characteristic length in Nusselt number definition
Nu	average Nusselt number
Q	input heat
T_s	temperature of liquid surface
ΔT	$T_w - T_s$
ΔT_{ec}	evaporator temperature minus condenser temperature
d	groove depth
g	gravitational constant
h_c	thermal convection coefficient
k	liquid thermal conductivity
ℓ_e	evaporator length
ℓ_x	length of heat pipe
ℓ_z	one-half of evaporator width
n	density of grooves
p_ℓ	liquid pressure
p_v	vapor pressure

$\Delta p_{x,visc}$	viscous pressure loss along EHD artery
q	input heat flux
q_{max}	maximum input heat flux
r_c	liquid radius of curvature
r_o	radius of curvature at groove entrance
$u(z)$	average liquid velocity in a groove
w	groove width
w_p	wetted perimeter
α	angle of heat pipe inclination
Δ	symbol denoting difference
ε_o	permittivity of free space
ε	dielectric liquid permittivity
θ	parameter defined in eq. (4.15)
λ	latent heat of vaporization
μ, μ_ℓ	liquid viscosity
ρ, ρ_ℓ	liquid density
σ	liquid-vapor surface tension

REFERENCES

[1] Jones, T. B., "The Feasibility of Electrohydrodynamic Heat Pipes, "NASA CR-114392, October, 1971, Colorado State University, Fort Collins, Colorado.

[2] Perry, M. P. and Jones, T. B., "Entrainment in Electrohydrodynamic Heat Pipes," NASA CR-114499, August 1972, Colorado State University, Fort Collins, Colorado.

[3] Jones, T. B. and Perry, M. P., "Experiments with an Electrohydrodynamic Heat Pipe," NASA CR-114498, September 1972, Colorado State University, Fort Collins, Colorado.

[4] Rohsenow, W. M. and Choi, H. Y-H, Heat, Mass, and Momentum Transfer, Prentice-Hall, Englewood Cliffs, New Jersey (1961), Section 7.3, pp. 142.

[5] Krieth, F., Principles of Heat Transfer, International Textbook Company, Scranton, Pennsylvania (1965), Section 8.4, p. 387.

[6] Clark, S. H. and Kays, W. M., "Laminar-Flow Forced Convection In Rectangular Tubes," ASME Transactions, Vol. 75, pp. 859-866 (1953).

[7] Schlichting, H. Boundary Layer Theory, McGraw-Hill Book Company, New York, New York (1960), Chapter XX, p. 517.

[8] Sabersky, R. H. and Acosta., A. J., Fluid Flow, Macmillan Company, New York, New York (1964), Section 1.2.

[9] Bressler, R. G. and Wyatt, P. W., "Surface Wetting Through Capillary Grooves," ASME Journal of Heat Transfer, Series C, Vol. 92, 1970. pp. 126-132.

[10] Jones, T. B., "An Electrohydrodynamic Heat Pipe," ASME 72-WA/HT-35 Winter Meeting, New York, New York. November, 1972.

[11] Perry, M. P. "Electrohydrodynamic Heat Pipe Experiments", MS Thesis, Department of Electrical Engineering, Colorado State University, Fort Collins, Colorado. June, 1973.